Electronic Supplementary Information

Hydroxylated Organic Semiconductors for Efficient Photovoltaics and Photocatalytic Hydrogen Evolution

Xuan Liu,[a] Yue Zhao,[a] Yongfeng Ni,[a] Fang Shi,[a] Xin Guo,*[a] and Can Li*[a]

[a] State Key Laboratory of Catalysis, Dalian Institute of Chemical Physics, Chinese Academy of Sciences, Dalian National Laboratory for Clean Energy, Dalian 116023, China.

* E-mail: guoxin@dicp.ac.cn, canli@dicp.ac.cn

Experimental Section

Materials and methods

The polymer PM6 and small-molecule BTP-4F were purchased from Solarmer Materials Inc. and Nanjing Zhiyan Technology Co., Ltd. Other intermediate materials were purchased from Aldrich, and Alfa and used without any further purification.

UV-Vis absorption spectra were recorded on a Cary 5000 UV-VIS-NIR spectrophotometer. Cyclic voltammetry (CV) was carried out on a CHI600D electrochemical workstation at a scan rate of 50 mV s^{-1} with an Ag/AgCl as the reference electrode. The tapping-mode AFM images were obtained by using a scanning probe microscope on a Bruker Metrology Nanoscope Ⅲ-D. ^{1}H-NMR and ^{13}C-NMR spectra were measured on a Bruker 400 MHz AVANCE III with tetramethylsilane as an internal reference. The mass spectroscopy (MS) was measured on an AB SCIEX MALDI-TOF/TOF 5800. The fourier infrared spectra (FTIR) were measured on FTIS

(Tensor 27) with different film thicknesses. The photoluminescence spectra were recorded by the fluorescence spectrometer (QM400, PTI). The two-dimensional grazing-incidence X-ray diffraction (2D GIXD) patterns were obtained using the beamline BL14B1 of the Shanghai Synchrotron Radiation Facility (SSRF) with the incident photon energy of 10 keV (wavelength of 1.2398 angstrom) at an incident angle of 0.14 ° and an exposure time of 60 s. The samples for the 2D GIXD measurement were prepared by spin-coating solutions on Si substrates. The deionized water was purified using a Milli-Q System. The hydrodynamic diameter of samples was measured by a Zetasizer Nano-ZS from Malvern Instruments. TEM of the samples was carried out with a HITACHI7700 TEM.

Fabrication and characterization of OPV devices

The photovoltaic devices were fabricated with a structure of glass/ITO/PEDOT:PSS/active layer/PDINO/Ag. The ITO-coated glass substrates were cleaned by deionized water, acetone, and isopropyl alcohol under ultrasonication for 30 min each and followed by a UV-ozone treatment for 20 min. Then, PEDOT:PSS (4083) layer was spin-coated (ca. 30 nm thick) onto the cleaned ITO surface. The substrates were then placed into an argon-filled glove box after being baked at 160 ℃ for 15 min. Subsequently, the active layer (PM6/BTP-4F: 16 mg mL^{-1} in total, 1:1.2, w/w, 0.5% 1-chloronaphthalene (CN) (v/v); PM6/BTP-FOH: 15.5 mg mL^{-1} in total, 1:1.3, w/w, 0.75% CN (v/v); PM6/BTP-2OH: 16.5 mg mL^{-1} in total, 1:1.5, w/w, 0.5% diphenyl ether (v/v) was spin-coated from a solution in chloroform at 3000 rpm for 30 s and annealed at 100 ^{o}C for 5 min. Then, PDINO in methanol solution was spin-coated at 3000 rpm for 30 s.

Finally, 120 nm Ag layer was deposited on the active layer under a high vacuum. The J-V measurement was performed via the solar simulator (SS-F5-3A, Enlitech) along with AM 1.5G spectra whose intensity was calibrated by the certified standard silicon solar cell (SRC-2020, Enlitech) at 100 mV cm^{-2}. The device area was 4.00 mm^{2}. The external quantum efficiency (EQE) data were obtained by using the solar-cell spectral-response measurement system (QE-R, Enlitech).

Fabrication of BHJ nanoparticles (NPs)

Individual stock solutions (0.50 mg mL^{-1}) of PM6, BTP-4F, BTP-FOH and BTP-2OH were prepared in chloroform. The solutions were heated at 50 °C for 2 h to ensure complete dissolution. The precursor solutions (4 mL) of nanoparticles were prepared from the stock solutions by mixing PM6 and each of BTP-4F, BTP-FOH or BTP-2OH with optimal weight ratios. Then, the precursor solution was added to a 0.5 wt% solution of TEBS in deionized water (16 mL), and stirred vigorously for 5 min. The mixed liquid was sonicated for 7 min with an ultrasonic processor (Fisher scientific FB120) to form a mini-emulsion. The mini-emulsion was heated at 85 ℃ for 30 min to remove the chloroform, and then filtered (0.45 μm) to remove any large aggregates, obtaining a surfactant-stabilized nanoparticle dispersion in water.

HER experiments

HER processes were conducted in a 45 mL quartz flask. The NPs composed of PM6 and each of BTP-4F, BTP-FOH or BTP-2OH (1 mg) in 0.2 M AA (12 mL) were loaded into a recirculating batch reactor (illumination area = 4.52 cm^{2}). The desired 15% loading ratio of Pt was achieved by adding 40 μL aqueous potassium hexachloroplatinate solution (3.81 mg mL^{-1} Pt). The reactor was evacuated and purged with Ar four times to remove O_2. All the suspensions with NPs were stirred and illuminated with 300 W Xe lamp (Ushio-CERMAX LX300) equipped with a mirror module (330-1100 nm). Gas samples were taken out by using a gas-tight syringe and run on a gas chromatograph (Shimadzu GC-8A, TCD, Ar carrier). Hydrogen was detected with a thermal conductivity detector referencing against standard gas with a known concentration of hydrogen. Any hydrogen dissolved in the reaction mixture was not measured and the pressure increase generated by the evolved hydrogen was neglected in the calculations.[1-5]

EQE measurements of the HER

EQE measurements were carried out in the same way as hydrogen evolution measurements, but with suitable band pass filters fitted to the light source. The sample was first illuminated under simulated solar light for 3 h to complete Pt photodeposition. Then, the reactor was evacuated and purged with Ar four times to remove all the H_2 evolved during this time. The light source was fitted with a band pass filter, and the BHJ NPs were illuminated with filtered light within a narrow wavelength range. The EQE was calculated using equation (1),

$$EQE(\%) = \frac{2nH_2}{nphotons} \times 100\% \tag{1}$$

where nH_2 represents the number of moles of H_2 evolved per hour and $nphotons$ represents the total number of photons incident on the sample surface (illumination area = 4.52 cm^2) per hour. The number of incident photons reaching the solution was measured using a calibrated Si photodiode (LS-100, EKO Instruments Co., LTD.).

Synthetic details

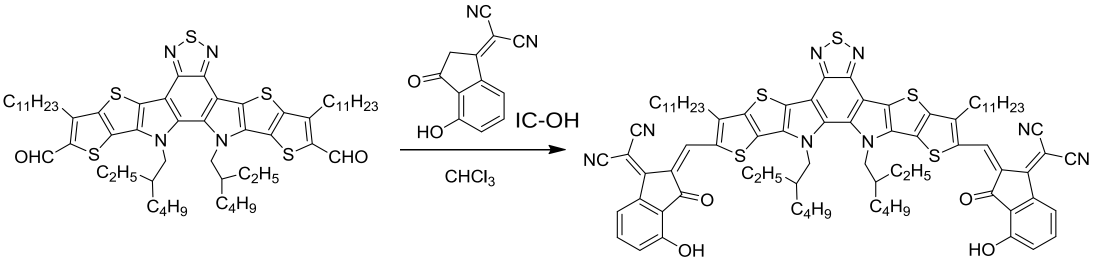

BTP-CHO BTP-2OH

Scheme S1. Synthetic route of BTP-2OH.

Synthesis of BTP-2OH: To a three-necked flask were added compounds BTP-CHO (102 mg, 0.1 mmol), IC-OH (132 mg, 0.6 mmol), chloroform (30 mL), and pyridine (1 mL). The mixture was protected with nitrogen and refluxed for 20 h. After cooling down to room temperature, the mixture was extracted with CH_2Cl_2 (100 mL), then washed with water (50 mL), dried over Na_2SO_4. The solvent was removed under reduced pressure and the residue was purified by column chromatography on silica gel using CH_2Cl_2 as eluent, yielding a dark blue solid (71 mg, 52%). ^{1}H NMR: (400 MHz, $CDCl_3$, δ): 9.23 (s, 2H), 9.06 (s, 2H), 8.10 (d, 2H), 7.55 (t, 3H), 7.12 (s, 2H). 4.72 (d, 4H), 3.14 (t, 4H), 2.04 (m, 2H), 1.81 (m, 4H), 1.44 (m, 4H), 1.19 (m, 32H), 0.97 (m, 12H), 0.79 (m, 6H), 0.63 (m, 12H). ^{13}C NMR: (101 MHz, $CDCl_3$, δ): 191.31, 160.24, 157.14, 153.21, 147.33, 144.93, 139.27, 137.52, 137.33, 135.55, 134.99, 133.72, 133.09, 130.22, 69.41, 55.67, 40.57, 31.91, 31.13, 29.87, 29.65, 29.62, 29.53, 29.50, 29.29, 23.39, 23.34, 22.90, 22.68, 14.07, 13.89, 13.86. HR-MS (MALDI-TOF): *m/z* calcd. for ($C_{82}H_{90}N_8O_4S_5$): 1410.5689. Found: 1410.5718.

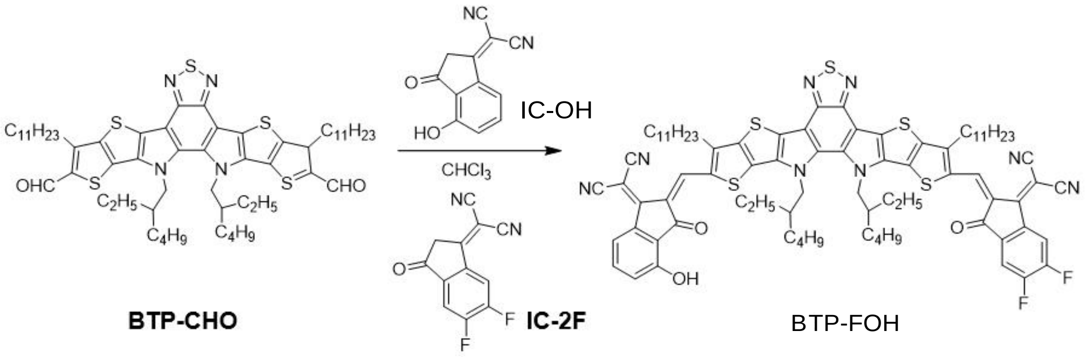

Scheme S2. Synthetic route of BTP-FOH.

Synthesis of BTP-FOH: The BTP-FOH was synthesized according to the same procedure as that of the BTP-2OH. The compounds BTP-CHO (102 mg, 0.1 mmol), IC-OH (22 mg, 0.1 mmol) and IC-2F (115 mg, 0.5 mmol) were used in this reaction, yielding a dark blue solid (59 mg, 43%). ^{1}H NMR (400 MHz, $CDCl_3$, δ): 9.30 (s, 1H), 9.17 (d, 2H), 8.58 (dd, 1H) 8.19 (d, 1H), 7.71 (t, 1H), 7.66 (t, 1H), 7.20 (s, 1H). 4.77 (d, 4H), 3.24 (t, 4H), 2.07 (m, 2H), 1.88 (m, 4H), 1.47 (m, 4H), 1.25 (m, 32H), 1.00 (m, 12H), 0.87 (m, 6H), 0.67 (m, 12H). ^{13}C NMR (101 MHz, $CDCl_3$, δ): 186.12, 153.92, 148.67, 147.51, 147.41, 144.99, 143.84, 136.94, 139.04, 135.25, 134.11, 133.35, 133.14, 130.65, 130.65, 130.44, 130.27, 129.32, 119.89, 115.17, 114.96, 114.56, 113.36, 113.13, 73.42, 55.37, 40.44, 31.91, 31.23, 30.45, 29.82, 29.62, 29.50, 29. 34, 23.18, 22.69, 14.12, 13.74, 13.67, 10.17. HR-MS (MALDI-TOF): *m/z* calcd. for ($C_{82}H_{88}F_2N_8O_3S_5$): 1430.5551. Found: 1430.5686.

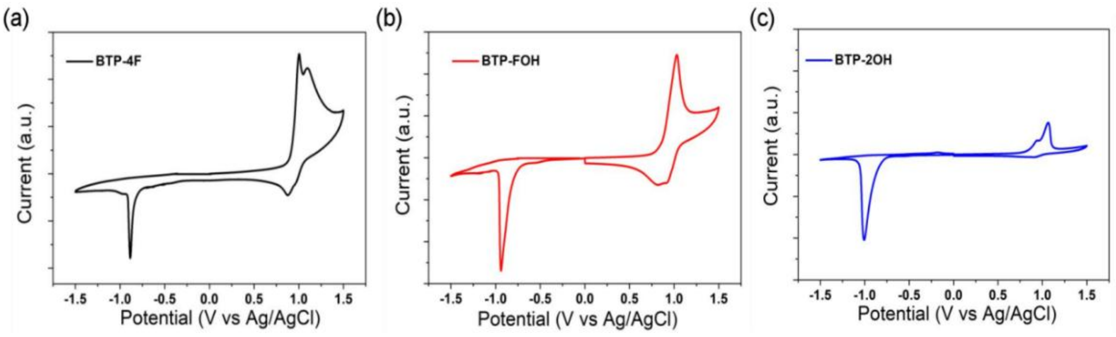

Fig. S1 Cyclic voltammetry (CV) curves of BTP-4F (a), BTP-FOH (b) and BTP-2OH (c). The HOMO and LUMO energy levels were determined by $E_{HOMO}= -(E_{onset,ox} - E_{Fc} +4.8)$ (eV) and $E_{LUMO}= -(E_{onset,red} - E_{Fc} +4.8)$ (eV), respectively; $E_{Fc}= 0.05$ eV.

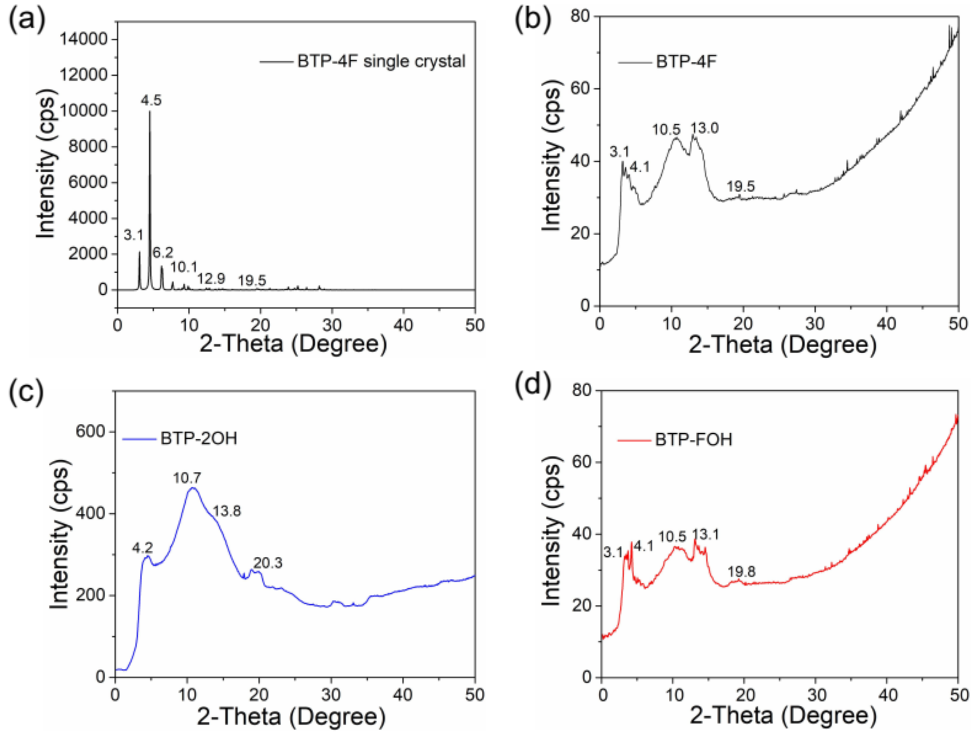

Fig. S2 XRD patterns for BTP-4F single crystal (a) and three acceptor powders (b-d). The stacking distances in Figure 2c in the manuscript are acquired via Bragg equation: $d=n\lambda/2\sin\theta$; the incident λ was 1.2 Å.

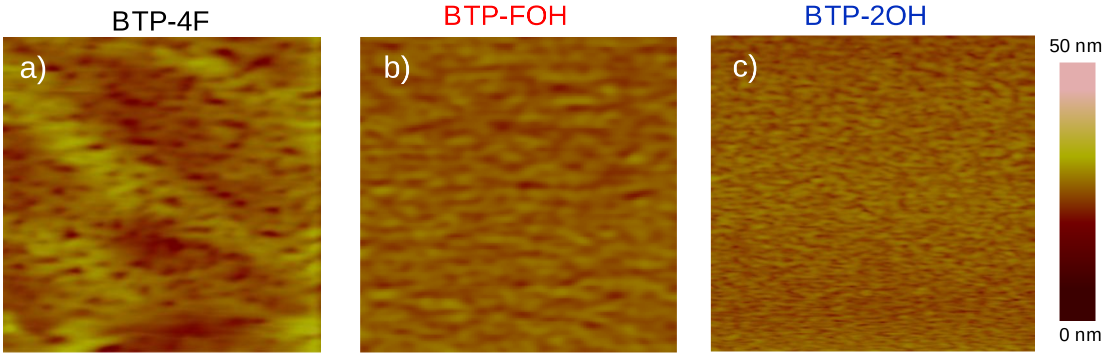

Fig. S3 AFM height images (2 μm×2 μm) of films of BTP-4F (a), BTP-FOH (b) and BTP-2OH (c).

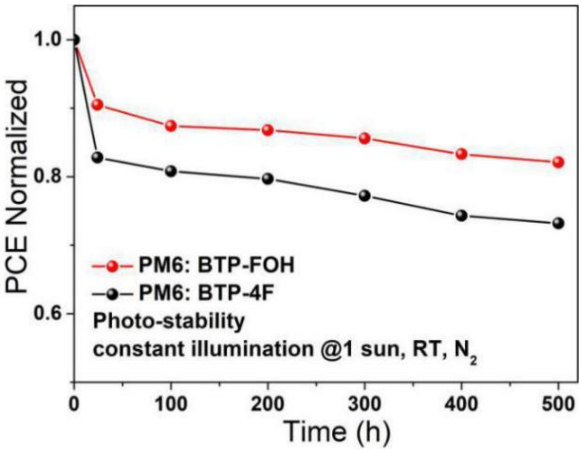

Fig. S4 Device stability of BTP-FOH and BTP-4F-based unencapsulated solar cells under light illumination (AM 1.5G, 100 mW cm^{-2}).

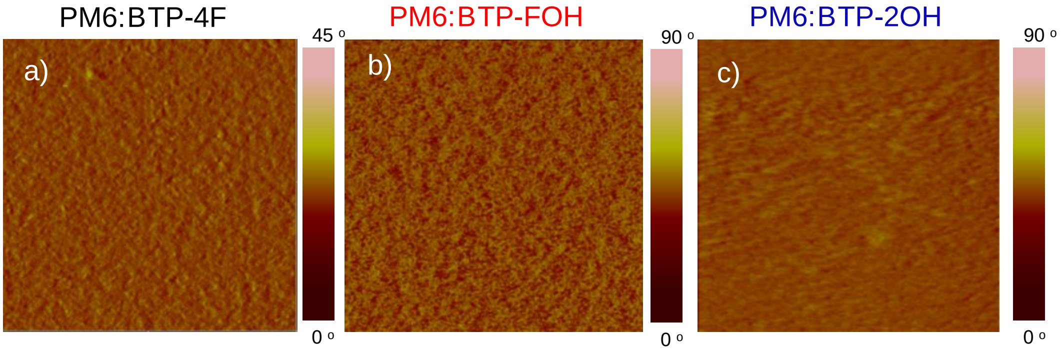

Fig. S5 AFM phase images (2 μm×2 μm) of PM6 blending films with BTP-4F (a), BTP-FOH (b) and BTP-2OH (c).

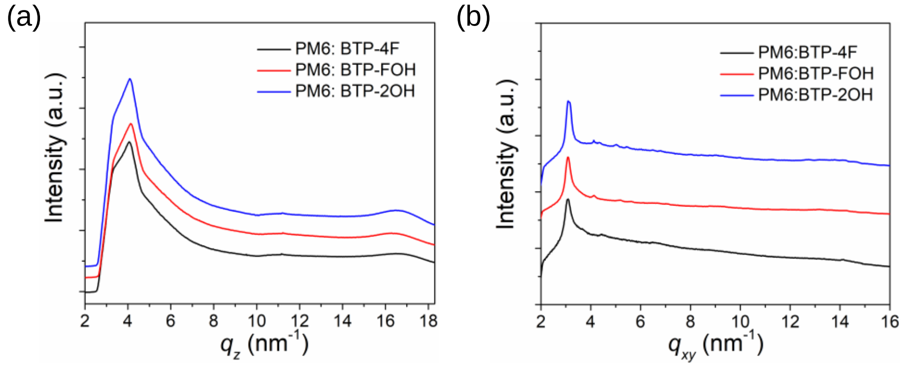

Fig. S6 (a) Out-of-plane (OOP) and (b) in-plane (IP) line cuts for the blend films based on PM6: acceptors.

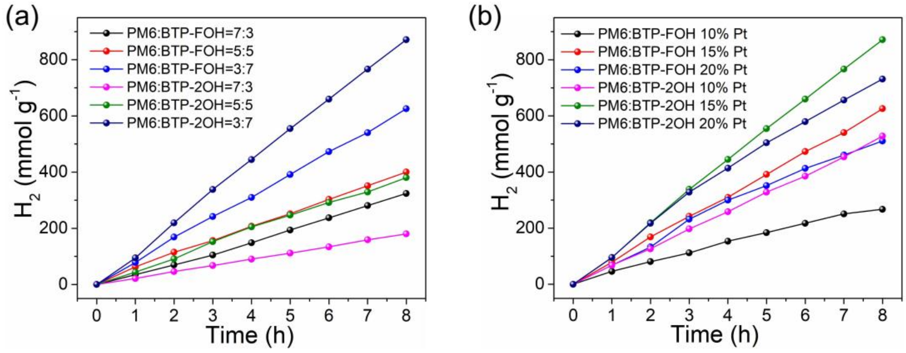

Fig. S7 (a) H_2 evolution versus time of nanoparticles formed with a range of PM6:BTP-FOH and PM6:BTP-2OH weight ratios. (b) H_2 evolution versus time of optimized NP photocatalysts (PM6:acceptors, 3:7) with varying Pt loading ratios.

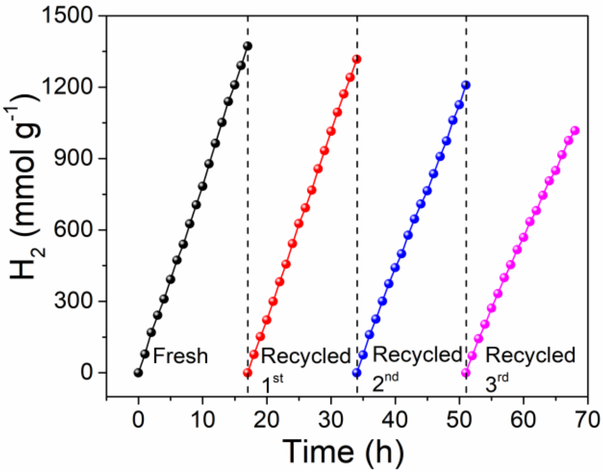

Fig. S8 H_2 evolution stability tests of PM6:BTP-FOH NPs loaded with 15% Pt for 68 h. For recycling experiments, the equivalent amount of AA is added after the end of every cycle, according to the consumption of AA.

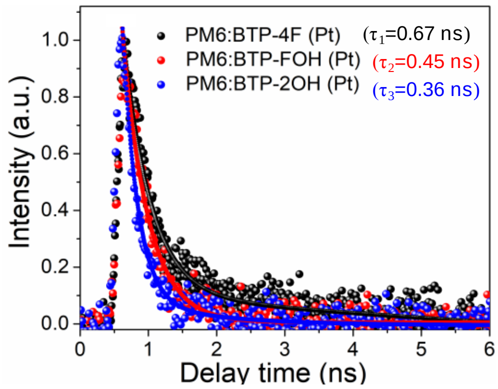

Fig. S9 TRPL results of PM6:BTP-4F, PM6:BTP-FOH, and PM6:BTP-2OH NPs with Pt loading. The three samples exhibit step-by-step reduced PL lifetimes with values of 0.67, 0.45, and 0.36 ns, respectively, revealing the more effective electron transfer to Pt after introducing more hydroxyl groups.

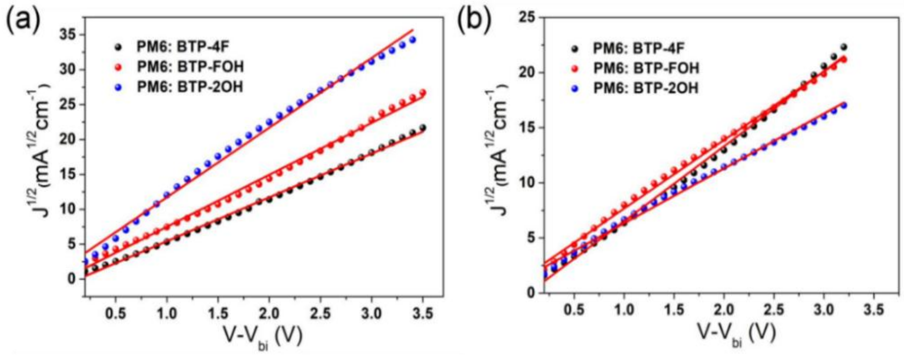

Fig. S10 $J^{1/2}$-V fitting results of the electron-only (a) and hole-only (b) devices based on PM6:acceptor blend films, measured by the SCLC method. The device structures for measurements of the hole and electron mobilities are ITO/PEDOT:PSS/active layer/MoO_3/Au and ITO/ZnO/active layer/PFN/Al, respectively. The J-V results were fitted using the Mott-Gurney law that includes field-dependent mobility, given by

$$J = \frac{9}{8}\varepsilon_0\varepsilon_r\mu_0\frac{(V - V_{bi})^2}{d^3}\exp(\beta\sqrt{\frac{V - V_{bi}}{d}})$$

where $\varepsilon_0\,\varepsilon_r$ is the dielectric permittivity of the active layer, d is the thickness of the active layer, μ_0 is the zero-field mobility, and β is the field activation factor.

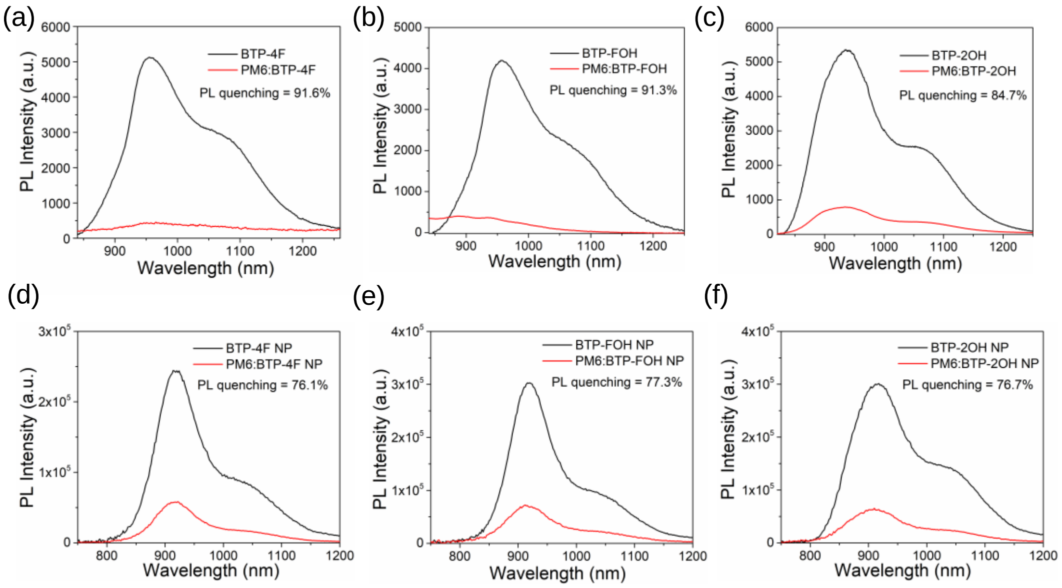

Fig. S11 PL quenching results of PM6:BTP-4F, PM6:BTP-FOH, and PM6:BTP-2OH in films (a-c) and NPs (d-f).

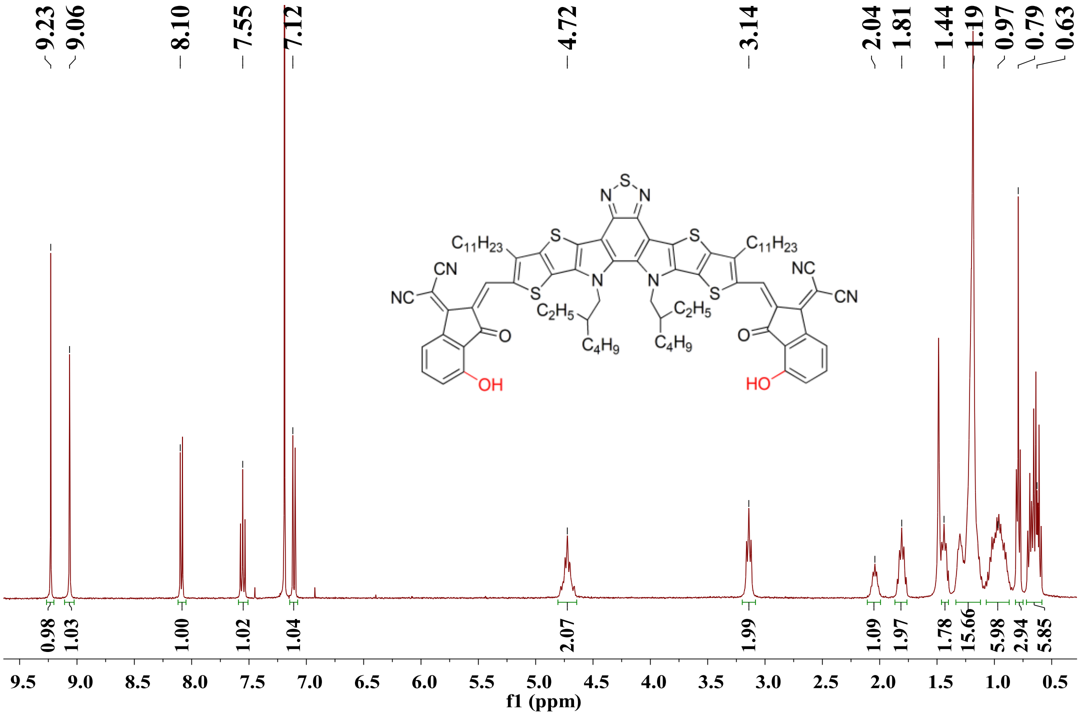

Fig. S12 ^{1}H NMR spectrum of compound BTP-2OH.

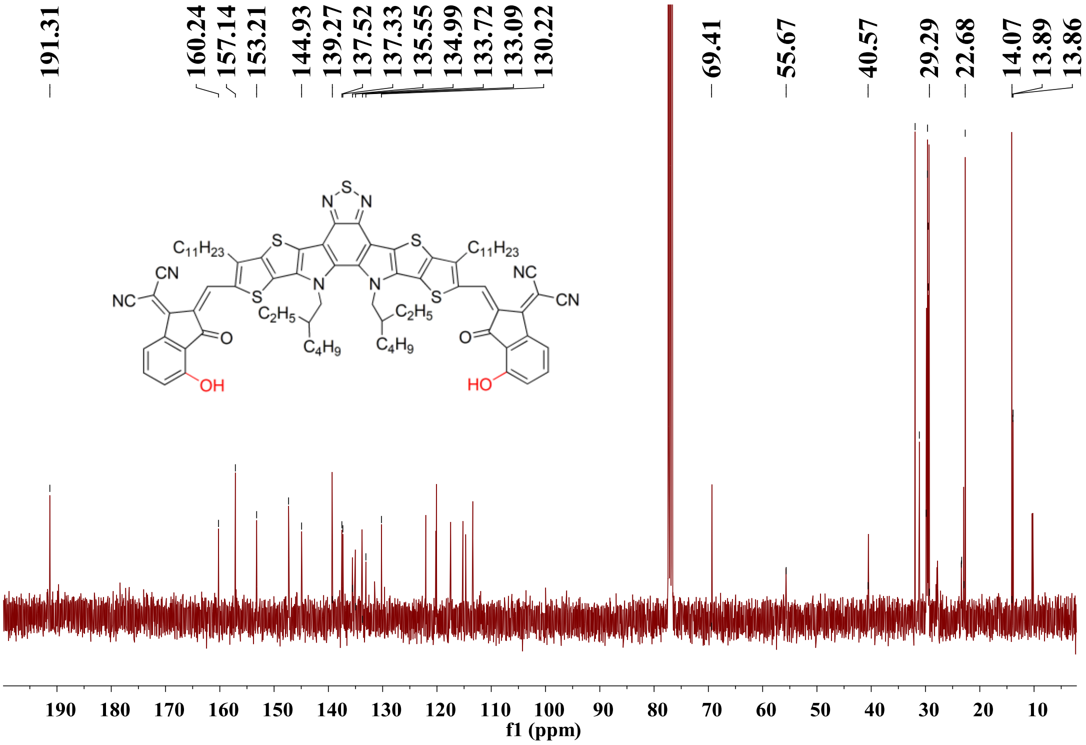

Fig. S13 ^{13}C NMR spectrum of compound BTP-2OH.

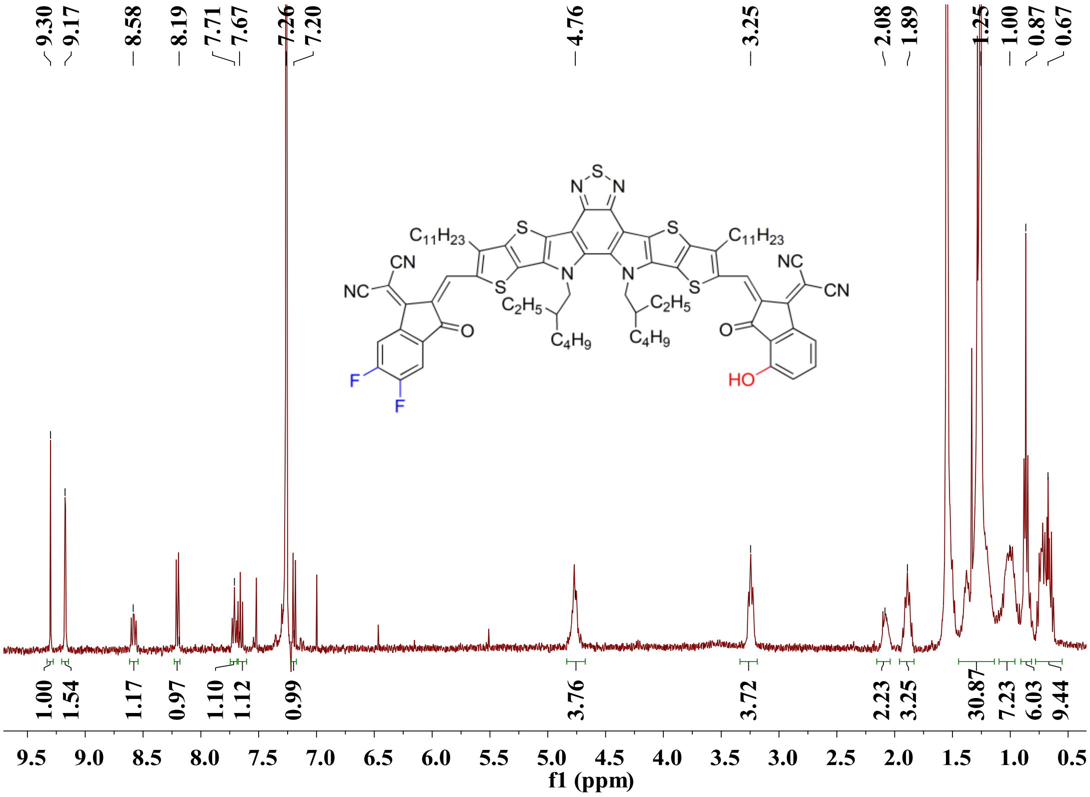

Fig. S14 ^{1}H NMR spectrum of compound BTP-FOH.

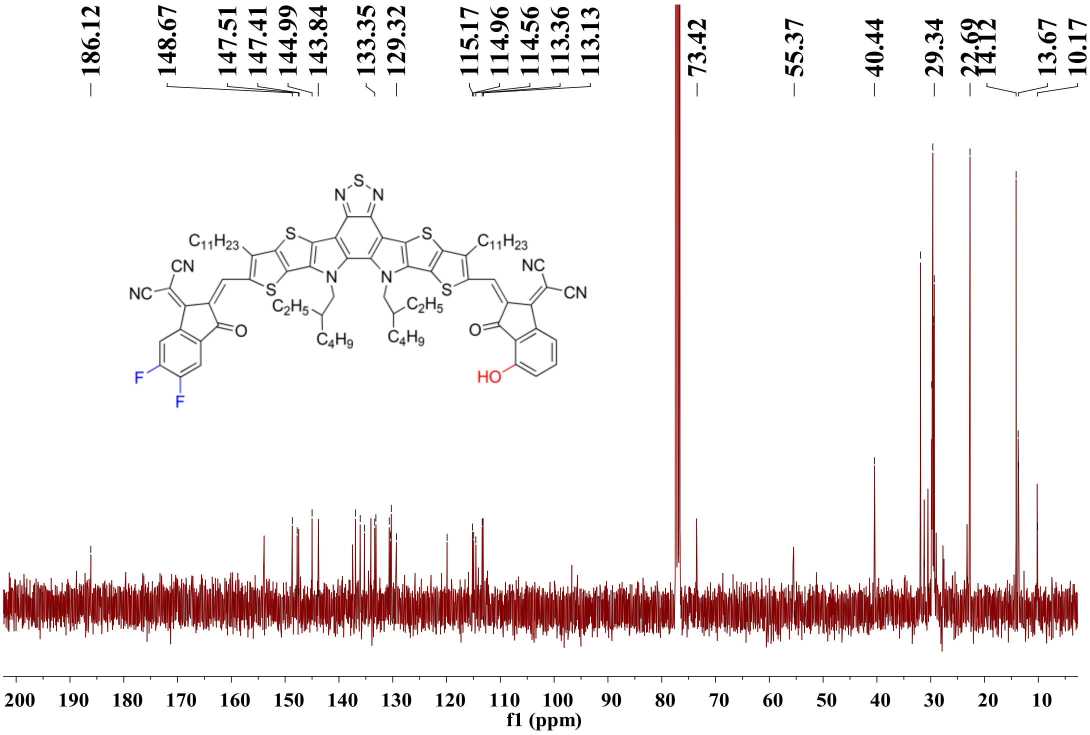

Fig. S15 ^{13}C NMR spectrum of compound BTP-FOH.

Table S1. Summary of high-performance BHJ NPs photocatalysts in recent years.

BHJ NPs	HOMO/LUMO of acceptor	Sacrificial reagent/cocatalyst	HER rate (mmol h^{-1} g^{-1})	EQE_{max} (%)	Ref
PTB7-Th/EH-IDTBR	-5.68/-4.08	AA/Pt	64.50	6.20 (700 nm)	3
PM6:$PC_{71}BM$	-6.10/-3.90	AA/Pt	73.70	8.70 (400 nm)	4
PM6:Y6	-5.90/-4.10	AA/Pt	43.90	5.00 (800 nm)	
PFBT/PFBODTBT/ITIC	-5.58/-3.86	AA/Pt	67.50	7.10 (600 nm)	5
PM6:TPP	-5.56/-3.89	AA/Pt	72.75	8.55 (800 nm)	6
PM6:Y6	-5.65/-4.10	AA/Pt	62.67	6.21 (800 nm)	
PM6:Y6CO	---/-3.98	AA/Pt	323.22[a]	11.58 (700 nm)[a]	7
PM6:Y6	-5.65/-4.10	AA/Pt	64.30	7.12 (800 nm)	This work
PM6:BTP-FOH	-5.60/-4.03	AA/Pt	78.40	8.35 (800 nm)	
PM6:BTP-2OH	-5.57/-3.98	AA/Pt	102.1	9.17 (800 nm)	

[a] These values were obtained based on a high Pt deposition amount with a K_2PtCl_6:BHJ NP ratio of 7:10 (*w*/*w*).

Table S2. Hole and electron mobilities of the PM6:acceptor-based blending films.

Sample	μ_e (cm^2 V^{-1} s^{-1})	μ_h (cm^2 V^{-1} s^{-1})	μ_e/μ_h
PM6:BTP-4F	4.26×10^{-4}	3.40×10^{-4}	1.25
PM6:BTP-FOH	5.12×10^{-4}	3.77×10^{-4}	1.35
PM6:BTP-2OH	9.16×10^{-4}	2.24×10^{-4}	4.09

References

1. H. Yang, X. Li, R. S. Sprick and A. I. Cooper, *Chem Commun*., 2020, **56**, 6790.
2. Y. Bai, L. Wilbraham, B. J. Slater, M. A. Zwijnenburg, R. S. Sprick and A. I. Cooper, *J. Am. Chem. Soc*., 2019, **141**, 9063.
3. J. Kosco, M. Bidwell, H. Cha, T. Martin, C. T. Howells, M. Sachs, D. H. Anjum, S. G. Lopez, L. Zou, A. Wadsworth, W. Zhang, L. Zhang, J. Tellam, R. Sougrat, F. Laquai, D. M. DeLongchamp, J. R. Durrant and I. McCulloch, *Nat. Mater*., 2020, **19**, 559-565.
4. J. Kosco, S. Gonzalez-Carrero, C. T. Howells, T. Fei, Y. Dong, R. Sougrat, G. T. Harrison, Y. Firdaus, R. Sheelamanthula, B. Purushothaman, F. Moruzzi, W. Xu, L. Zhao, A. Basu, S. D. Wolf, T. D. Anthopoulos, J. R. Durrant and I. McCulloch. *Nat. Energy*, 2022, **7**, 340-351.
5. A. Liu, L. Gedda, M. Axelsson, M. Pavliuk, K. Edwards, L. Hammarström and H. Tian, *J. Am. Chem. Soc*., 2021, **143**, 2875-2885.
6. Z. Zhang, W. Si, B. Wu, W. Wang, Y. Li, W. Ma and Y. Lin, *Angew. Chem. Int. Ed*., 2022, **61**, e202114234.
7. Y. Liang, T. Li, Y. Lee, Z. Zhang, Y. Li, Z. Liu, C. Zhang, Y. Qiao, S. Bai, Y. Lin, *Angew. Chem. Int. Ed.* 2023, **62**, e202217989